



# Flow-rate limitation in a uniform thin-walled collapsible tube, with comparison to a uniform thick-walled tube and a tube of tapering thickness<sup>☆</sup>

C.D. Bertram\*, N.S.J. Elliott

*Graduate School of Biomedical Engineering, University of New South Wales, Sydney, NSW 2052, Australia*

Received 12 December 2001; accepted 21 August 2002

## Abstract

Previous experiments on a tapered-thickness tube showed qualitatively different behaviour from that exhibited by a uniform thick-walled tube. To understand whether the taper or the thinner wall was responsible, similar aqueous flow-limitation experiments were conducted on a uniform thin-walled tube of the same material, with all other experimental set-up the same. As in the thick tube, there was a dramatic reduction in flow-rate when collapse and flow limitation started, but during external pressure reduction, the limited flow-rate progressively increased, so that as in the tapered-thickness tube, there was little flow-rate increase when collapse ceased. Hysteresis was thus a prominent feature of the relationship between flow-rate and pressure drop along curves of constant upstream transmural pressure. Flow-rate limitation was mainly accompanied by large-amplitude self-excited oscillation for both increasing and decreasing external pressure, to an even greater extent than in the tapered-thickness tube. Clusters of points sharing the same pair of upstream transmural pressure and upstream driving pressure values were found, indirectly implying as in the tapered-thickness tube that the flow-limited flow-rate for a given pressure drop was not uniquely determined by upstream transmural pressure. Negative effort dependence was observed in all three tubes, but in the thin tube, as in the tapered-thickness tube, it was obscured for some values of upstream transmural pressure where low-frequency single-collapse-per-cycle oscillations occurred. Thus, the qualitatively unique properties of the tapered-thickness tube appear to be confined to the relative lack of hysteresis, and the oscillatory regime in which collapse ceased before the downstream end. The rest of the observed behaviours seem to be characteristic simply of more compliant tubing.

© 2003 Elsevier Science Ltd. All rights reserved.

## 1. Introduction

From the experimental point of view, a collapsible tube is any tube with sufficiently flexible walls that it can elastically (reversibly) accommodate deformation to a highly noncircular cross-section when external pressure exceeds internal pressure. The deformation includes two landmarks: first buckling from a reasonably circular shape, and first contact between the opposite inside walls. Between these, the compliance of the tube is much greater than either when the tube is distended or when it is collapsed beyond first contact. When there is flow through the tube, the high compliance allows the flow to affect markedly the shape of the tube, so that the flow and the boundary configuration are strongly coupled. This leads to the behaviour known as flow-rate limitation, whereby the flow-rate through the tube becomes

<sup>☆</sup> Presented in part at the IUTAM Symposium 'Flow in Collapsible Tubes and Past Other Highly Compliant Boundaries', University of Warwick, 26–30 March 2001.

\*Corresponding author. Tel.: +61-2-9385-3928; fax: +61-2-9663-2108.

E-mail address: [chrisb@gsbme.unsw.edu.au](mailto:chrisb@gsbme.unsw.edu.au) (C.D. Bertram).

substantially independent of the pressure downstream when that pressure is low enough to cause collapse at the downstream end of the tube.

Collapsible-tube flow-rate limitation is studied largely because it occurs in the human body. Naturally occurring instances are in the systemic veins, where venous return to the heart is limited, in the pulmonary airways, where maximum expiratory airflow-rate is thus set, and in the urethra, where flow-rate during micturition is limited. Many other instances beyond these few examples can be listed (Shapiro, 1977; Bertram, 1995); in addition, many diagnostic or therapeutic medical procedures induce collapse of vessels that do not collapse naturally.

When the Reynolds number of the flow exceeds about 250, or rather more in thicker tubes, another consequence of the flow/boundary coupling is the potential for self-excited oscillation. Laboratory experiments on flow-rate limitation have previously been conducted (Bonis and Ribreau, 1978; Gavriely et al., 1989) at flow-rates where such oscillation is possible, but the extent to which oscillation does or does not accompany flow-rate limitation has not always been considered.

Our first experiments in this area were conducted on a thick-walled silicone-rubber tube corresponding to those used in our previous work on pressure-drop limitation and other aspects of collapsible-tube dynamics. In this uniform tube, it was found (Bertram and Castles, 1999—hereinafter referred to as ref. I) that at the onset of flow-rate limitation (defined as where flow-rate no longer increased with pressure drop under conditions of constant upstream transmural pressure), flow-rate decreased greatly from the maximum achieved previously. Flow-rate limitation was seldom accompanied by large-amplitude self-excited oscillation; the latter was mostly exhibited only during the transition to or from maximum flow to the flow-limited state. There was hysteresis: flow-rate at a given driving head depended not just on upstream transmural pressure but also on its history. When rising to certain values of upstream transmural pressure (by reduction of external pressure), either flow-rate limitation or an absence of collapse could be obtained, depending on starting point.

We subsequently applied similar techniques of investigation to a tube of tapering wall thickness (increasing in the streamwise direction). Such tubes are of interest because they imitate the longitudinally varying stiffness of physiological conduits, as experienced for instance by expiratory airflow. From the stand-point of the experimenter, a tapered-stiffness tube can under some conditions collapse only as far as an intermediate site, whereas a uniform tube always collapses first and most close to the downstream end.

In the tapered-thickness tube (Bertram and Chen, 2000—hereinafter referred to as ref. II), flow-limited operating points ranged over all modes and control-space regions of self-excited oscillation. There was no dramatic reduction in flow-rate at the onset of flow-rate limitation. For certain combinations of head and upstream transmural pressure, multiple operating points, representing slightly differing flow-rates, were found. It was further shown that these clusters represented true nonuniqueness of flow-rate for a given pair of up- and downstream transmural pressures. A new family of weak oscillation modes was observed, corresponding to throat locations remote from the usual downstream end of the tube. In these modes, the location of the throat (defined as the most collapsed point, and also always the epicentre of tube wall oscillation) itself oscillated, and further slight minima of tube area were perceptible upstream of the throat.

Thus the two previous investigations have shown up a number of qualitative differences in behaviour between the thick-walled uniform tube and the tapered-stiffness tube. The latter was made from a segment of the former tubing by machining away part of the wall thickness; thus its longitudinally averaged stiffness was much less than that of the uniform tube. Were the different behaviours caused by the taper or by the reduced stiffness? On the face of it, qualitative differences in behaviour would not be expected to arise from a quantitative difference in stiffness, so the taper seemed more likely to be responsible.

The purpose of this investigation was to answer the question posed above, by studying the aqueous flow-limitation behaviour of a uniform thin-walled collapsible tube. All other aspects of the experiments were similar to those used previously, thus allowing us to compare the behaviour with that of the two other tubes of similar internal diameter previously studied in this laboratory: the uniform thick-walled tube, and the tube with wall thickness varying linearly along its length. The thick-walled tube had the same wall thickness as the downstream end of the tapered tube, while the thin-walled tube approximated the wall thickness of the upstream end; thus the two uniform tubes straddled the longitudinally varying stiffness of the tapered tube (which had constant internal diameter).

The qualitative similarities and differences between the behaviours of the three tubes in particular shed light on which aspects of behaviour are indeed characteristic of or possibly unique to tapered-stiffness tubes. As will be seen, many of the behaviours first observed in the tapered stiffness tube have now also been observed in the thin-walled uniform tube, and therefore seem to be related to reduced stiffness.

## 2. Methods

In all but a handful of details, the methods corresponded to those used in our previous investigations of flow-rate limitation (refs. I and II); this description will therefore be brief, and readers are referred to those papers for further detail. A detailed description is also given by Elliott (2000).

The silicone-rubber tube was 1.0 mm thick (measured by vernier caliper); its unstressed mid-wall diameter was 13.0 mm (calculated from circumference as the average measured width of a cut-open segment), implying inside and outside diameters of 12.0 and 14.0 mm. However, the intact tubing assumed an oval cross-section, with major and minor outside diameters of 10.0 and 16.5 mm. As usual, it was mounted at the axial strain induced by an axial force of 3.14 N; this strain would have been somewhat greater than that induced by the same load on the previous tubes. The elastic modulus of the material was measured in separate measurements of axial tube strain to be 3.15 MPa; this compares with 3.8 MPa for the thick-walled tube. The difference is attributed to the fact that the thin-walled tubing came from a different manufacturer. Using the Poisson ratio measured for the material of the thick-walled tube (Bertram, 1987), these data lead to a normalising pressure unit based on flexural rigidity for the thin tube of 1.17 kPa, to be compared with 11.3 kPa<sup>1</sup> for the thick tube. The unsupported length of the tube was 228.2 mm, corresponding to 19.0 inside diameters.

The upstream and downstream flow conditions are crucial in setting the dynamics of the collapsible tube. Here, the same conditions applied as in the experiments of refs. I and II; these in turn corresponded to those set by Bertram et al. (1990), who used three different values of downstream flow resistance; that used here, as in refs. I and II, was the lowest of those values ( $R_2^I$  as defined in 1990).

As before, we first mapped out control space in  $(p_u, \bar{p}_{e2})$ -coordinates, where  $p_u$  is the upstream flow-driving pressure,  $p_e$  the pressure external to the collapsible tube,  $p_2$  the pressure at the downstream end of the tube,  $\bar{p}_2$  is the time average of  $p_2$ , and  $\bar{p}_{e2} = p_e - \bar{p}_2$ . In these experiments,  $p_e$  was varied incrementally, keeping  $p_u$  constant, and the locations of boundaries between regions of distinct tube behaviour were found. Four values of  $p_u$  up to 100 kPa were initially investigated; higher values than this would have risked damaging the tube during violent self-excited oscillations. Later, two additional  $p_u$ -values (50 and 83 kPa) were added to give extra resolution, but only  $\bar{p}_{e2}$ -values corresponding to  $\bar{p}_{e1}$ -values of interest for the flow-rate limitation experiments were investigated ( $p_1 =$  pressure at the upstream end of the tube); region boundaries were not sought. As before, all experiments for incremented  $p_e$  were repeated while decrementing  $p_e$ , and the two sets of observations were plotted separately in view of the hysteresis exhibited by both silicone rubber itself and the dynamical system.

For the flow-rate limitation investigations,  $p_u$  was fixed at one of the six chosen values between 13 and 100 kPa, and  $p_e$  was either incremented or decremented, pausing at and recording all operating points corresponding to a  $\bar{p}_{e1}$ -value of interest. Having thus found the approximate coordinates corresponding to transition to or from flow-rate limitation for each  $p_u$ , we found the precise start of the transition by incrementing/decrementing  $p_u$  by 1 kPa at a time, and making the corresponding  $p_e$  adjustment to regain the desired value of  $\bar{p}_{e1}$ . The resulting constant- $\bar{p}_{e1}$  curves were plotted in  $(\bar{Q}, \bar{p}_{12})$ -coordinates ( $\bar{Q} =$  flow-rate), with separate diagrams for increasing and decreasing  $p_e$ .

### 3. Results

#### 3.1. Waveforms

The thin tube oscillated with an even greater repertoire of periodic modes than the thick-walled tube, which first showed the richness of this dynamical system. Fig. 1 shows a collation of these oscillations, arranged in a logical order according to our previous classification scheme, which however had to be extended to cover what was observed here. As before, we observed low-frequency (L) oscillations of types U and D, denoting a  $p_2$ -waveform spending either most of the cycle above a line halfway between its extremes (U), or at least half of the cycle below that line (D). As  $p_e$  was increased, LU tended to become LD. We also distinguished between cycles having different numbers of  $p_2$ -minima. At  $p_u = 100$  kPa, for example, as  $p_e$  increased, LU became LU2, indicating collapse twice in quick succession in each cycle.<sup>2</sup> The combination of these trends yielded such progressions as LU3 → LD4, then LD4 → LD5 → LD6. The amplitude of the smaller collapses within each collapse cycle tended to decrease, until they reached a point where they were deemed *minuscule* (LDm) and too small to count. The ‘r’ in LDmr and LDr modes signifies a distinctively *rounded* waveform. With still further  $p_e$  increase, the tube collapsed along its whole length and oscillated at high (H) frequencies ( $\approx 45$  Hz) with very large amplitude ( $\approx 165$  kPa peak-to-peak). These oscillations were eventually overwhelmed by the pressure external to the tube and the tube assumed a continuously collapsed state with steady flow (c). At some operating points in the c region,  $p_2$  was unsteady, exhibiting rapid small noise-like fluctuations. When the standard

<sup>1</sup>This number for the thick-walled tube differs from the 10.9 kPa given by Bertram (1987), because slightly different measured values for the diameter and wall thickness were used, as well as a different method of slope determination.

<sup>2</sup>The notation LU2, etc., here is not the same as  $U_2$ , etc. (Bertram and Butcher, 1992a) or  $I_2$ , etc. (Bertram and Castles, 1999), where the suffix was used simply to denote a second (etc.) region of U or I oscillation in ascending order of  $\bar{p}_{e2}$ .

deviation of these exceeded 0.5 kPa, state c was instead termed nf; extremely localised tube-wall flutter is believed largely responsible, in conjunction with fluctuations induced by the turbulent flow.

### 3.2. Control space

Fig. 2(a) shows how all these states were fitted into a systematic scheme with the help of the control-space diagram. Where strictly control space would have  $(p_u, p_e)$ -coordinates, we use  $\bar{p}_{e2}$  instead of  $p_e$  to allow inclusion of the zones of divergent instability (marked UN—unattainable by the protocol followed) that separate many of the states. The boundaries forming closed regions are constructed from the columns of observations at discrete  $p_u$ -values by conservative linear interpolation, linking qualitatively similar modes at different  $p_u$ -values. In comparison with the corresponding diagram for the thick-walled tube (ref. I), a greater number of different oscillatory modes was seen here. This made it more difficult to complete the region boundaries. For instance, the unattainable zone separating the LU2 and LU3 modes at  $p_u = 100$  kPa became a smooth transition at  $p_u = 66$  kPa, and LU (i.e., LU1) oscillations did not appear at  $p_u = 33$  kPa. The change from LU to LD-type oscillations was a continuous gradual process, therefore

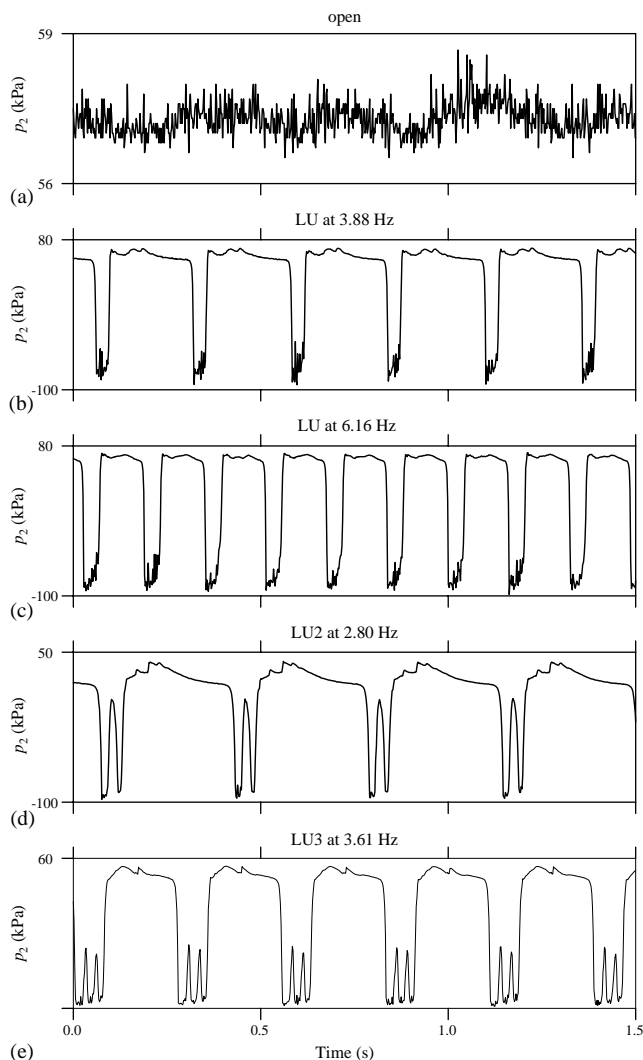


Fig. 1. Waveform examples of the many different types of flow-induced oscillation and other states observed in the thin-walled silicone rubber tube. The trace depicted is in every case pressure at the downstream end of the tube. The mode descriptor is shown above the respective panel, along with the frequency of oscillation where appropriate. See text for explanation of the modes. Continued on pages 12, 13 and 14.

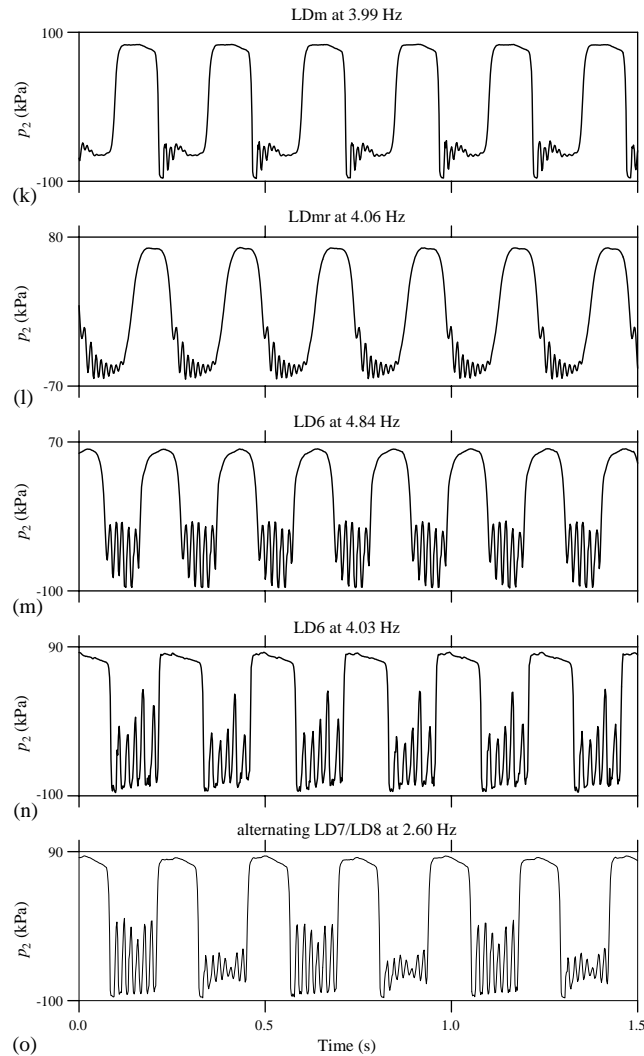


Fig. 1 (continued).

smooth boundaries like that linking the LU4→LU5 transition at  $p_u = 66$  kPa with the LD4→LD5 transition at  $p_u = 100$  kPa were appropriate. Along this boundary the LU5-type oscillations were separated from the LD5-type oscillations midway between  $p_u = 66$  and 83 kPa, because only LU5 was observed at  $p_u = 66$  kPa and only LD5 was observed at  $p_u = 83$  kPa.

Fig. 2(b) shows the corresponding control space for decreasing  $p_e$ . This was qualitatively somewhat similar to that for increasing  $p_e$ , although not all of the modes found during ascent reappeared during descent, while some regions (e.g., H) were enlarged; quantitatively virtually all of the region boundaries shifted. (The thick-walled tube investigated previously behaved oppositely, in that the control-space diagram included more oscillatory regions when  $p_e$  was being reduced than when augmented; see ref. I.) All unattainable zones disappeared at  $p_u = 100$  kPa other than the largest one separating the LU and o modes. In both the thick-walled uniform tube and the tapered-thickness tube, nf-mode points were predominantly at the high- $p_u$  end, whereas here the fluctuations reached the defined nf-mode threshold at points scattered without apparent order in the low- $p_u$  part of the space. Apart from these small-amplitude (relative to the periodic oscillation modes) noisy traces, the recordings from the thin-walled tube were notable for the almost complete absence of such aperiodic oscillations as had been observed in the thick-walled tube (Bertram et al., 1991). However, while descending the  $p_u = 100$  kPa column, one point was observed where the tube alternated intermittently between I (at 12.01 Hz) and LU (at 6.33 Hz) oscillations.

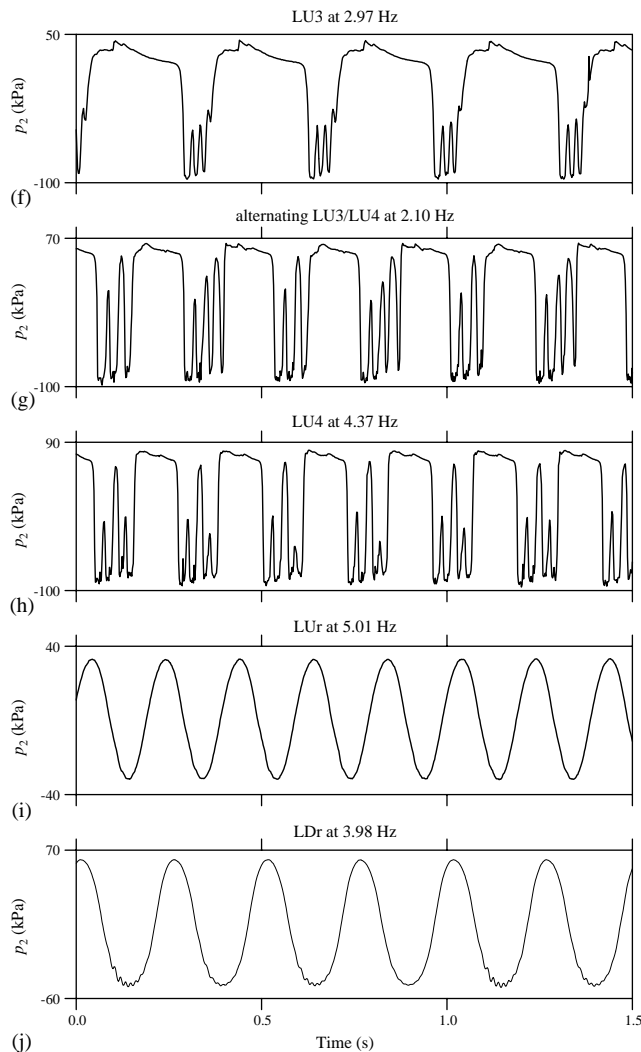


Fig. 1 (continued).

### 3.3. Flow-rate limitation

Fig. 3(a) shows the tube exhibiting flow-rate limitation, when curves of constant  $\bar{p}_{e1}$  are plotted in  $(\bar{Q}, \bar{p}_{12})$ -space. Nine such curves are shown, all for increasing  $p_e$ , spanning the  $\bar{p}_{e1}$ -range  $-3.5$  to  $+4.0$  kPa. At  $-3.5$  kPa, the tube never reached flow-rate limitation; higher  $p_u$  than the allowed maximum of 100 kPa would have been necessary. At 3.0 and 4.0 kPa, flow-rate was already limited through tube collapse at the lowest  $p_u$  of 13 kPa. Thus, the range of interest here was from  $-3.5$  to 3 kPa; in the thick-walled tube it was from 30 to 50 kPa, and 6 to 11 kPa in the tapered tube. These ranges are consistent with the average bending stiffness of the tubes; that is, for a given value of  $p_u$ , the minimum  $\bar{p}_{e1}$ -value at which  $\bar{Q}$  was substantially independent of  $\bar{p}_{12}$  decreased with the average bending stiffness of the tube.

Six curves in Fig. 3(a) display the dramatic transition to flow-rate limitation in which flow-rate is sharply reduced relative to that pertaining before the onset of collapse. In the most exaggerated case ( $\bar{p}_{e1} = -3$  kPa), the flow-limited flow-rate is only some 27% of that reached before collapse. This behaviour is akin to that exhibited by the thick-walled tube, as was the 'negative effort dependence', whereby  $\bar{Q}$  actually dropped as  $\bar{p}_{12}$  increased. However, the thin tube parted company from the thick one in that the majority of flow-limited operating points were oscillatory, as can be seen by the symbol annotations for mode (also shown, as a number, is the  $p_u$ -value). In the thick tube, with few exceptions flow-limited points were nonoscillatory (c or nf), all oscillatory regions of control space having been crossed over during

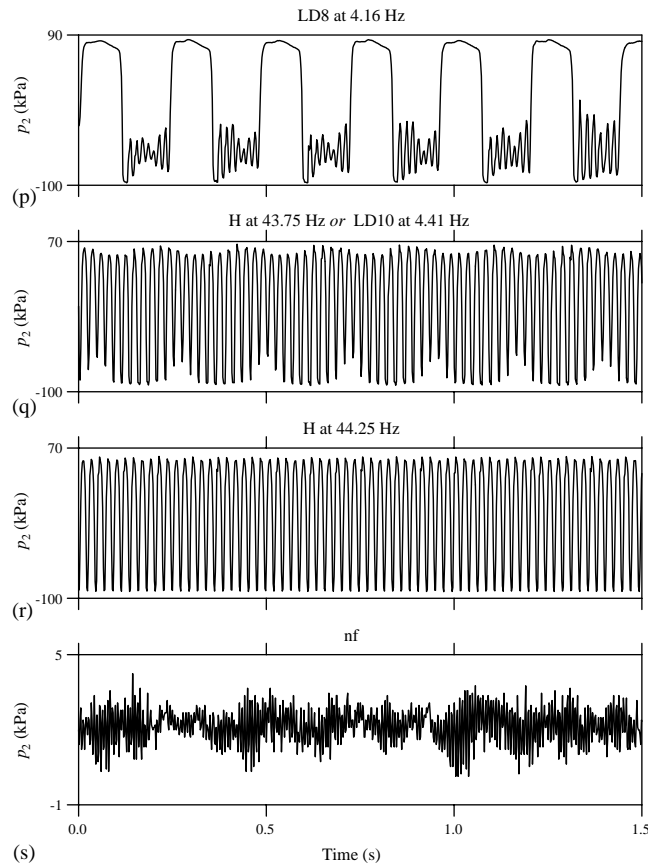


Fig. 1 (continued).

the transition to flow-rate limitation. This transition is essentially a discontinuity in the constant- $\bar{p}_{e1}$  curve. To the resolution of our experiments (increments of 1 kPa in  $p_u$ ), transition was unstable; there were no points along the line of transition which had the required  $\bar{p}_{e1}$ -value, in either uniform tube, for increasing  $p_c$ .

The prevalence of oscillatory flow-limited points in the thin tube can be understood by superimposing these observations on the previously established control-space diagram as in Fig. 4(a). This is a comparison of data from two different experiments, therefore slight problems of mis-registration occur, such that points apparently stray into unattainable zones. Interpretation of the superimposition at fine scale is not profitable as a result, but overall patterns can be perceived. As in the thick tube, transition takes the operating point almost vertically up, but whereas in the thick tube transition ends in the  $c/nf$  region, here it ends still in the upper reaches of the oscillatory modes. Only those curves ( $\bar{p}_{e1} = 3$  or 4 kPa) where flow-rate is limited for all  $p_u$ -values start above the oscillatory modes. Once flow-rate limited, all the curves run essentially parallel to each other, diagonally upwards in control space. In the present tube, the gradient of this slope is less than the slope of the upper margin of the oscillatory regions, so that all the constant- $\bar{p}_{e1}$  curves eventually become oscillatory as  $p_c$  increases. In contrast, the corresponding plot for the thick tube (Fig. 6, ref. I) showed that the two slopes were essentially the same; at low  $p_u$ , the constant- $\bar{p}_{e1}$  curves were above the oscillatory regions, as here, but by virtue of this property they stayed above at higher  $p_u$ -values. Indeed if one includes the tapered-stiffness tube in this comparison (Fig. 4(a), ref. II), it can be seen that the average gradient of the flow-rate-limited part of the constant- $\bar{p}_{e1}$  curves (plotted as  $\bar{p}_{e2}$  vs.  $p_u$ ) decreased, relative to the gradient of the uppermost closed region of control space, with the average bending stiffness of the tube.

The flow-limitation behaviour of the thin tube differed somewhat when  $\bar{p}_{e1}$  was approached from above, by reduction of  $p_c$ , as seen in Fig. 3(b). Most notably,  $\Delta\bar{Q}$  for the transition from flow-rate limitation to open-tube steady flow was far smaller and it did not increase in magnitude monotonically with decreasing  $\bar{p}_{e1}$ . Negative effort dependence was exhibited but this became obscured towards the middle of the  $\bar{p}_{e1}$  series, with the  $-5.0$  kPa curve having the largest deviation from 'normal' behaviour, i.e. flow-rate that is inversely related to pressure drop. In fact, the  $\bar{p}_{e1} = -5.0$  kPa

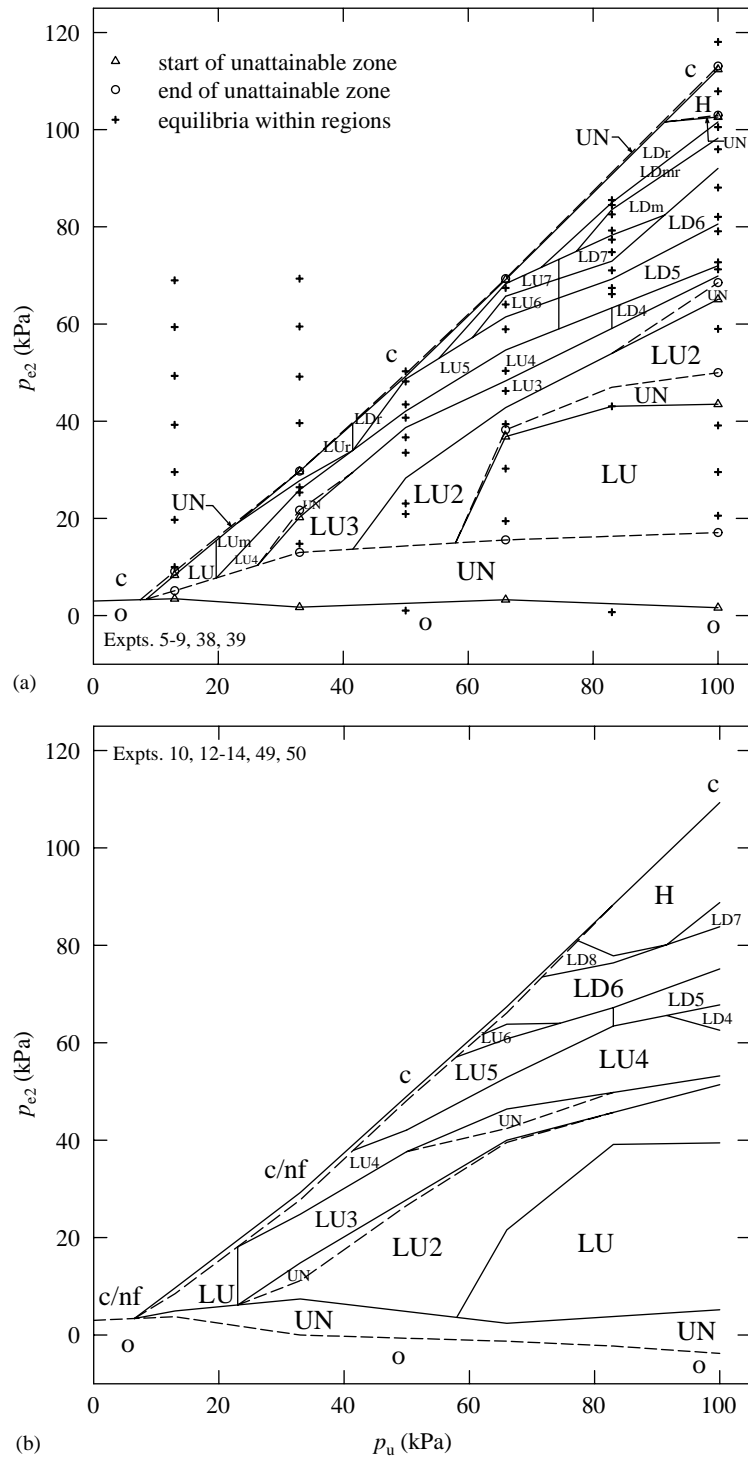


Fig. 2. The behaviour modes are shown mapped out in the modified control space defined by  $(p_u, \bar{p}_{e2})$ -coordinates. The region boundaries are constructed by conservative interpolation linking observations at certain  $p_u$ -values while  $p_{e2}$  is either (a) increased or (b) decreased. System hysteresis demands that these observations be kept separate. The construction process is made explicit in (a) by showing the locations of the three types of observations by symbols; in the final stage as represented by (b), the symbols are omitted.



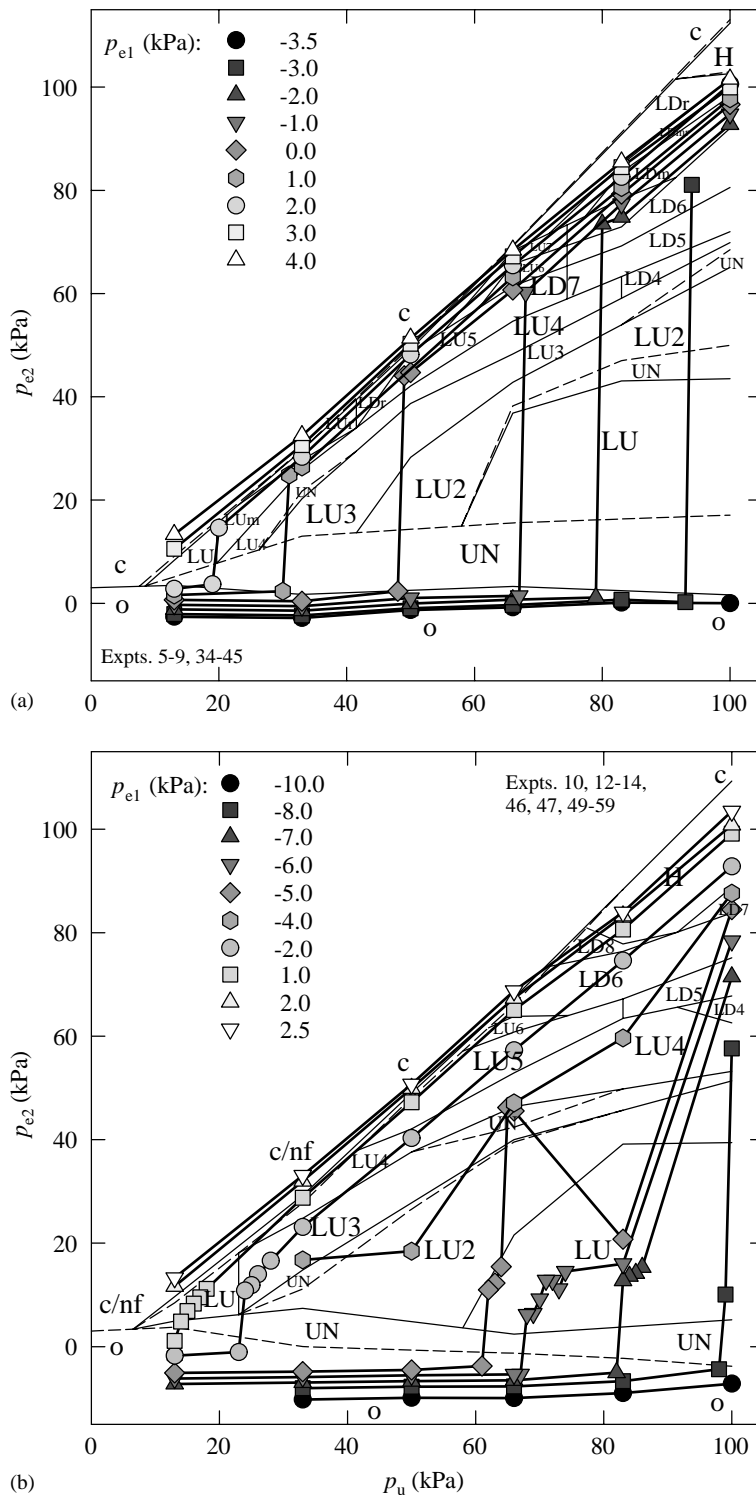


Fig. 4. The constant- $\bar{p}_{e1}$  curves of Fig. 3 are shown replotted in the modified control space, overlaid on the mode region boundaries established in the experiments leading to Fig. 2, for (a) increasing and (b) decreasing  $p_e$ .

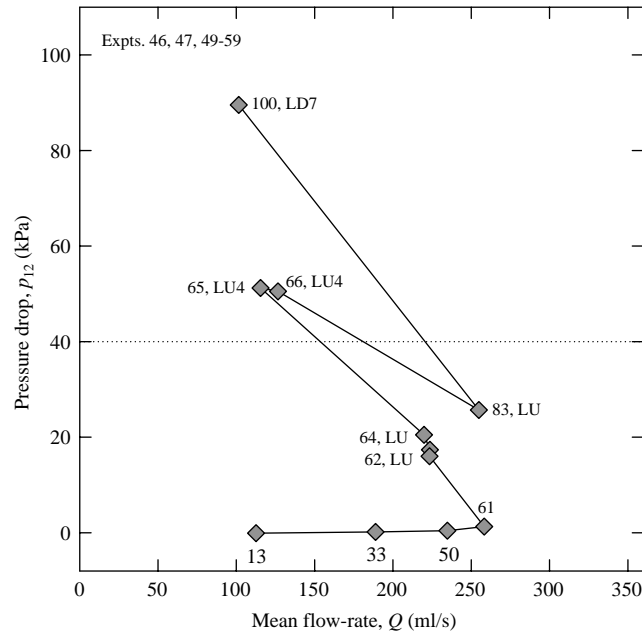


Fig. 5. The isolated  $\bar{p}_{e1} = -5$  kPa curve from Fig. 3(b). Nonuniqueness is demonstrated by the three intersection points of the flow-limited part of the curve with the  $\bar{p}_{12} = 40$  kPa dotted line.

curve is special in that the flow-limited flow-rate was not uniquely determined by  $\bar{p}_{e1}$ . As described in ref. II, this can be shown by drawing a horizontal line (in Fig. 3(b)) at a given  $\bar{p}_{12}$ -value and finding more than one flow-rate for a single  $\bar{p}_{e1}$ ; Fig. 5 illustrates the case of  $\bar{p}_{e1} = -5.0$  kPa where up to three flow-limited flow-rates can be found. The issue of nonuniqueness will be revisited below.

Each of the  $\bar{p}_{e1}$  values investigated in Fig. 3(b) was reached by first increasing  $p_e$  until  $\bar{p}_{e1} = 20$  kPa, at which point the tube was in a steady collapsed state (c), and then descending to the required target value. The range of  $\bar{p}_{e1}$  values necessary to cover the curves of interest (that is, always flow-limited, never flow-limited, and those in between over the range of  $p_u$  investigated here) spanned from  $-10$  to  $+2$  kPa. Referring to Fig. 3(a), one can see that over the whole range of  $p_u$ ,  $p_e$  can be increased until  $\bar{p}_{e1} = -3.5$  kPa and the tube will remain in an open steady state. Therefore, if  $-3.5$  kPa was the starting value of  $\bar{p}_{e1}$  before descending to the target value, flow-rate limitation would be absent for all  $\bar{p}_{e1}$  values less than  $-3.5$  kPa; from Fig. 3(b) these would be  $\bar{p}_{e1} = -10.0, -8.0, -7.0, -6.0, -5.0$  and  $-4.0$  kPa. A direct demonstration of the extent of this hysteresis is afforded by plotting for both increasing and decreasing  $p_e$  just the two curves from Figs. 3(a) and (b) for a given  $\bar{p}_{e1}$ -value, for instance  $-2$  kPa, as shown in Fig. 6. A similarly profound hysteresis was found in the flow-rate limitation exhibited by the thick-walled tube (Fig. 9, ref. I). However, in the tapered-stiffness tube, the  $\bar{p}_{e1}$  values which demonstrated both flow-limited flow-rates and lack thereof at the same  $p_u$  were limited to just 3 and 4 kPa.

The collection of points grouped together in the ellipse at the lower right side of Fig. 3(b) can be better explained with the use of a control-space diagram, as in Fig. 4(b). There would appear to be two different dynamical behaviour patterns present: (i) the curves  $\bar{p}_{e1} = 2.5, 2, 1$  and  $-2$  kPa, which exhibited flow-rate limitation behaviour analogous to  $\bar{p}_{e1} = 4, 3, 2$  and  $1$  kPa, respectively from Fig. 3(a) when  $p_e$  was being increased; and (ii) the curves  $\bar{p}_{e1} = -6, -7$  and  $-8$  kPa, which began in the low-frequency multiple-collapse-per-cycle LDn regions and then dropped dramatically to the LU region, where they persisted almost until the start of the LU  $\xrightarrow{\text{UN}}$  o unattainable zone, at which point they dropped to the open steady state. The intermediate  $\bar{p}_{e1}$  values,  $-4$  and  $-5$  kPa, display a behaviour which conforms to (i) at some points and (ii) at others. In the case  $\bar{p}_{e1} = -5$  kPa, the tube went from LU4 at  $p_u = 65$  kPa to LU at  $p_u = 64$  kPa, which change was accompanied by a large drop in  $\bar{p}_{e2}$  and  $\bar{p}_{12}$ , and a large increase in  $\bar{Q}$  (see Fig. 3(b) for  $\Delta\bar{p}_{12}$  and  $\Delta\bar{Q}$ ).

### 3.4. Nonuniqueness

The tapered-stiffness tube was previously shown (ref. II) to exhibit nonunique flow-rates for a given combination of  $\bar{p}_{e1}$  and  $\bar{p}_{12}$ . Such behaviour is intimately tied up with the form of the relation between  $p_e$  and  $\bar{p}_{e1}$ , which, since it depends

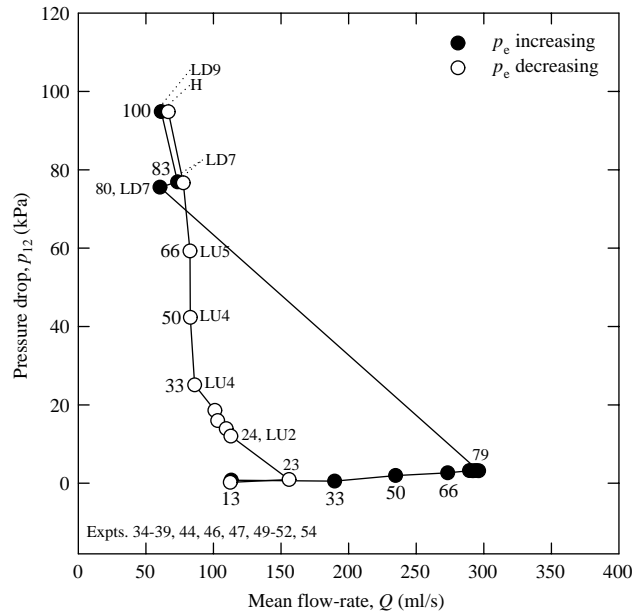


Fig. 6. Hysteresis in the flow limitation behaviour is highlighted by plotting the curves for  $\bar{p}_{e1} = -2$  kPa from Figs. 3(a) (increasing  $p_e$ ) and (b) (decreasing  $p_e$ ).

on  $p_u$ , is actually a family of curves. In the present investigation, this relation was initially established through the experiments leading to the control-space diagrams. Subsequently, the flow-rate limitation experiments provided a second set of data, this time at the specific  $\bar{p}_{e1}$ -values of Fig. 3. Fig. 7 shows the relation obtained from these data, as a series of constant- $p_u$  curves on  $(p_e, \bar{p}_{e1})$ -axes. Each of the  $\bar{p}_{e1}$ -values investigated for flow-rate limitation purposes is indicated by a horizontal line; the curves were completed making use of the data from the earlier series of experiments, and a dotted symbol distinguishes points added in this way [full details of the procedure are given by Elliott (2000)].

Traversing a constant- $\bar{p}_{e1}$  (dotted) line in Fig. 7(a) from left to right, points of intersection with the constant- $p_u$  curves are encountered, with the value of  $p_u$  increasing to the right, i.e., with  $p_e$ . Due to the nonmonotonic nature of the  $(p_e, \bar{p}_{e1})$  relation, sometimes a  $\bar{p}_{e1}$  line intersects the same  $p_u$  curve more than once. For instance, consider  $\bar{p}_{e1} = -2$  kPa. Initially, the  $p_u = 13$  kPa curve is met and the tube is open. Approaching the  $p_u = 33$  kPa curve, the first point of intersection again corresponds to the open-tube state. These two points can also be located in Figs. 3(a) and 4(a). However, if  $p_u$  is held constant and  $p_e$  is increased further, then the tube collapses, causing  $p_{e1}$  to fall dramatically as the tube assumes the LU3 mode. This transition corresponds to the  $\overset{\text{UN}}{\circ}$  LU3 unattainable zone in Fig. 4(a) at  $p_u = 33$  kPa. However, since the value of  $\bar{p}_{e1}$  has now changed, no  $\bar{p}_{e1} = -2$  kPa operating point can be recorded in the LU3 region. Continuing to increase  $p_e$  allows  $\bar{p}_{e1} = -2$  kPa to be re-attained, but the operating point thereby shifts to the LU4 region. Only these two valid intersections with the  $p_u = 33$  kPa curve occur; there is a third, middle one between the constant- $\bar{p}_{e1}$  line and the negative-slope part of the constant- $p_u$  curve, but this does not represent a stable point. The dual intersection defines a means of ‘pre-transition’ from open-tube steady flow to flow-rate limitation that is an alternative to the transition for  $\bar{p}_{e1} = -2$  kPa shown in Fig. 3(a). Although such pre-transitions were not specifically noted in the tapered-stiffness tube, similar behaviour to that shown in Fig. 7(a) was observed (Fig. 6 of ref. II).

The situation at  $p_u = 50$  kPa is similar to that described for  $p_u = 33$  kPa, except that there exist three intersections, the first with the tube open, and the other two being low-frequency oscillations of type LU3 and LU4, respectively. Now from Fig. 3(a), we observe that the transition to flow-rate limitation for  $\bar{p}_{e1} = -2$  kPa occurs between 79 and 80 kPa. While the tube could remain open at  $p_u = 79$  kPa (and satisfy  $\bar{p}_{e1} = -2$  kPa), when  $p_u$  was increased to 80 kPa, the first possible point at which  $\bar{p}_{e1} = -2$  kPa was attained involved flow-rate limitation. Therefore, when approaching the  $p_u = 83$  kPa curve in Fig. 7(a) along the  $\bar{p}_{e1} = -2$  kPa (dotted) line, oscillations break out before intersection occurs. The first and only intersection is necessarily then accompanied by self-excited oscillation, in the LD7 mode (see Fig. 3(a)). The same situation occurs at  $p_u = 100$  kPa with LD9 oscillations. The shape of the constant- $p_u$  curves in Fig. 7(a) is such that if there is more than one intersection, the first intersection is *always* with the tube open.

This whole sequence of events for  $\bar{p}_{e1} = -2$  kPa is shown in Fig. 8(a), plotted as  $\bar{p}_{12}$  vs.  $\bar{Q}$ . The main solid curve is the same as that found in Fig. 3(a), but since all points in the figure belong to the same  $\bar{p}_{e1}$ , the additional points that make

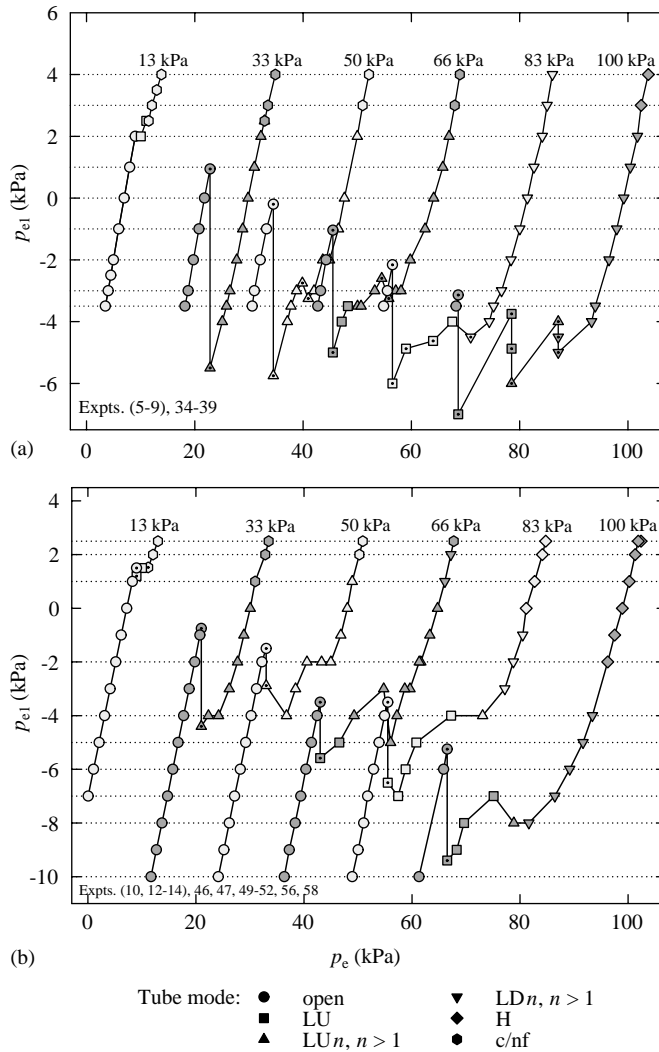


Fig. 7. The nonmonotonic dependence of  $\bar{p}_{e1}$  on  $p_e$ , when  $p_e$  was being (a) increased and (b) decreased, at the six constant  $p_u$ -values indicated by the annotations. Symbols represent by shape the tube mode, and are shaded or not to make clear to which  $p_u$ -value they pertain; those with a central dot show derived values (see text).

up the multiple intersections in Fig. 7(a) are also connected by thinner continuous lines to this curve, via paths determined by their oscillatory mode and the  $p_u$ -value. Each set of points from Fig. 7(a) which shares the same  $(p_u, \bar{p}_{e1})$  coordinates is interconnected by dashed lines. The remaining (solid) paths were added according to the following logic. The three LU4 points at  $p_u = 33, 50$  and  $66$  kPa were clearly closely related; the top one was then joined to the sole (LD7) flow-limited point at the next higher  $p_u$  investigated ( $80$  kPa). At some point between  $p_u = 33$  and  $50$  kPa along the LU4–LU4 line, there was necessarily a bifurcation where the LU3 mode originated, with half-way along the LU4–LU4 line being the most conservative choice in the absence of further data. Similarly, this LU3 mode disappeared somewhere between  $p_u = 50$  and  $66$  kPa.

Fig. 8(a) clearly demonstrates that flow-limited flow-rate is not uniquely determined by upstream transmural pressure. For example, consider the case when the pressure drop is  $40$  kPa. If one constructs the horizontal line  $\bar{p}_{12} = 40$  kPa, it is found to intersect the solid lines three times. The first two intersections correspond to flow-limited flow with LU4 and LU3 oscillation, respectively. The third intersection is at the transition from open steady flow to flow-limited flow. The transition is unsteady in the sense that  $\bar{p}_{e1} = -2$  kPa was not regained until the transition was complete, therefore any such intersections do not represent attainable points for  $\bar{p}_{e1} = -2$  kPa. So for this example of

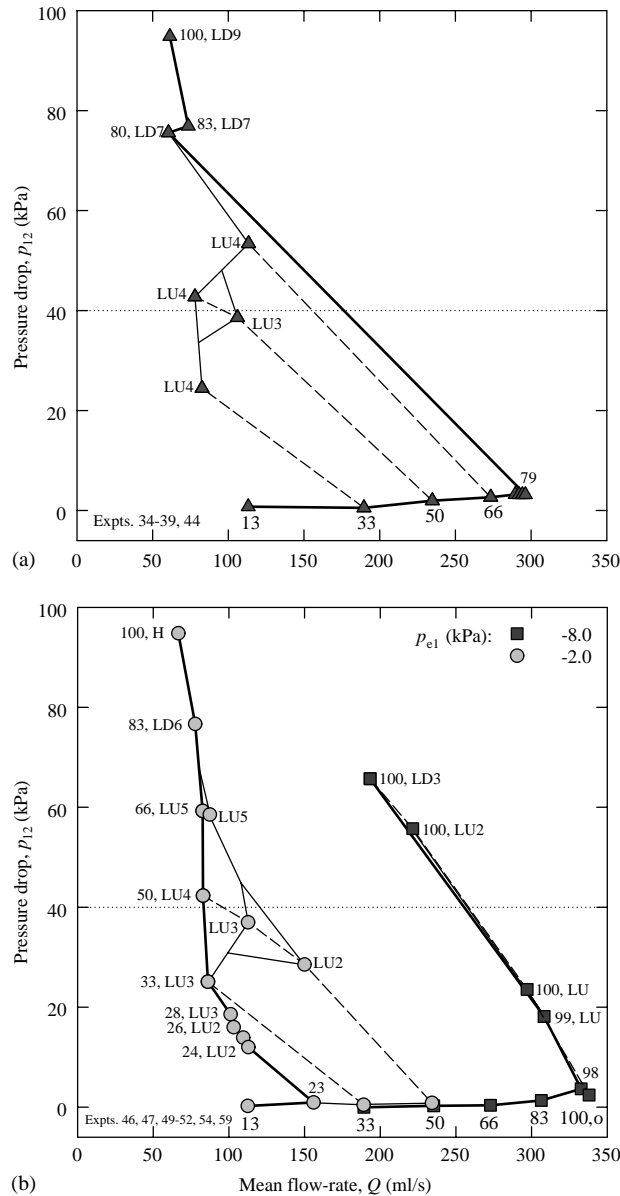


Fig. 8. Flow-rate limitation at  $\bar{p}_{e1} = -2$  kPa, demonstrating nonuniqueness, for (a) increasing  $p_e$ , (b) decreasing  $p_e$ —the latter also shows  $\bar{p}_{e1} = -8$  kPa. The bold lines illustrate the traditional route to flow limitation as shown previously in Figs. 3(a) and (b), respectively. Dashed lines join points of equal  $p_u$ -value. See text for construction process of the thinner continuous lines.

$\bar{p}_{12} = 40$  kPa, there are two flow-limited flow-rates available at the one pair of values of  $\bar{p}_{e1}$  and  $\bar{p}_{12}$ ; this defines nonuniqueness.

One may argue that the LU3 and LU4 points do not qualify for inclusion on the figure, as the transition to flow limitation has not yet occurred. However, the dashed lines in Fig. 8(a) at  $p_u = 33, 50$  and  $66$  kPa themselves are all possible pre-transitions to flow limitation, which actually occur only if one goes substantially above the chosen  $\bar{p}_{e1}$ -value before regaining it, as in Fig. 7. The solid line at  $79/80$  kPa represents the last juncture at which transition could take place, under the protocol of increasing  $p_u$  by  $1$  kPa at a time and adjusting  $p_e$  to regain the requisite  $\bar{p}_{e1}$ .

If the seven flow-limited points in Fig. 8(a) were all present on the control space of Fig. 4(a) (only the uppermost three are), they would lie just below the top of the net of closed oscillatory regions, along a sloping line which is an extension of one of the family of such lines actually shown in Fig. 4(a). If one were to extrapolate this extended line

from  $p_u = 33$  kPa back downwards to the point where it intersected the lowermost unattainable zone (at around  $p_u \approx 20$  kPa and  $\bar{p}_{e2} \approx 10$  kPa), this point would represent the earliest possible onset of flow-rate limitation at  $\bar{p}_{e1} = -2$  kPa by any conceivable protocol. Since all the similar sloping lines in Fig. 4(a) are so close together, earliest possible onset of flow-rate limitation at any  $\bar{p}_{e1}$ -value occurs in approximately the same location.

Fig. 7(b) presents the relation between  $p_e$  and  $\bar{p}_{e1}$  when  $p_e$  was being reduced. Again, as with Fig. 7(a), in order to complete the diagram a handful of additional points, identified by symbols with a central dot, were derived from control-space experiments. Using again the example of  $\bar{p}_{e1} = -2$  kPa, one traverses the diagram horizontally, but this time from right to left. The  $p_u = 100$  and 83 kPa curves are intersected once each, corresponding to tube modes H and LDn (LD6, see Fig. 3(b)), respectively. Although it is difficult to see from the figure, because the two data points were virtually coincident, there are actually two LUn-type intersections at  $p_u = 66$  kPa (both LU5). Further travel to the left yields four intersections at  $p_u = 50$  kPa (three of type LUn and the last one when the tube was open), two at 33 kPa (LUn and open) and a single intersection at  $p_u = 13$  kPa (open).

All of these intersection points are plotted as  $\bar{p}_{12}$  vs.  $\bar{Q}$  in Fig. 8(b), together with the analogous points for  $\bar{p}_{e1} = -8$  kPa as a comparison. Following the principles established for Fig. 8(a), sets of points sharing the same values of  $\bar{p}_{e1}$  and  $p_u$  have been connected with dashed lines, and the points are then interconnected with solid lines based on their tube mode. If one cuts the figure horizontally at an appropriate location, multiple flow-limited flow-rates are indicated at a single pair of  $\bar{p}_{12}$  and  $\bar{p}_{e1}$  values. For example, sectioning the  $\bar{p}_{e1} = -2$  kPa curve at  $\bar{p}_{12} = 40$  kPa yields three distinct flow-limited flow-rates. Therefore, the property of nonuniqueness extends to both increasing and decreasing  $p_e$  for the thin-walled collapsible tube.

#### 4. Discussion

The major finding of this investigation is that a nonunique relation between upstream transmural pressure and flow-limited flow-rate is *not* a feature peculiar to tapered-stiffness tubes. In a uniform thin-walled tube, as many as three distinct flow-limited flow-rates were possible at the same values of pressure drop and upstream transmural pressure. The transition to flow-rate limitation was in general achieved through a large reduction in flow-rate. An extremely rich variety of periodic self-excited oscillation modes was observed, and many of these modes accompanied flow-rate-limited states. Negative ‘effort dependence’ was seen, i.e., reduction in flow-limited flow-rate as pressure drop increased. Under flow-rate-limiting conditions, when the external collapsing pressure was being decreased there appeared to be two distinct trends in the relation between pressure drop and flow-rate: one trend at low values of upstream transmural pressure ( $\bar{p}_{e1}$ ) which involved single-collapse-per-cycle oscillations and another at higher values of  $\bar{p}_{e1}$ , associated with oscillations that had multiple collapses within each cycle. At an intermediate upstream-transmural-pressure value the flow-limitation behaviour switched between the two trends. These results are now discussed in depth and compared both to the previous work by Bertram and colleagues (I, II) on aqueous flow limitation and to analogous findings of other investigators. Particular reference is made to the air-flow experiments of Patel (1993), which document nonuniqueness, and of Gavriely et al. (1989), which show schematically the prevalence of oscillation during flow-rate limitation.

##### 4.1. Self-excited oscillations

Following the method established by Bertram et al. (1991), the initial stage of investigation involved the construction of control-space diagrams, which define closed regions of behaviour mode and zones of unattainability in  $(p_u, \bar{p}_{e2})$  coordinates; the hysteresis of the dynamical system meant that separate diagrams were needed for increasing and decreasing  $p_e$  (Figs. 2(a) and (b), respectively). The control-space diagram is particularly useful as it provides a convenient map of all the possible oscillatory behaviour of the tube, which can be used to explain the transition from steady to unsteady flow.

The control-space diagrams show several noteworthy features. Before collapse, the tube is open (o) and the flow steady. An unattainable zone (UN) separates the open mode from regions of low-frequency self-excited oscillations. This zone is divergently unstable since when approaching it from above or below (by increasing or decreasing  $p_e$ ),  $\bar{p}_{e2}$  jumps from one side to the other. After collapse, the reduced cross-sectional area brings about a large pressure drop down the length of the tube, causing  $\bar{Q}$  and thus  $\bar{p}_2$  to reduce significantly, and  $\bar{p}_{e2}$  to increase. This jump in  $\bar{p}_{e2}$  (either positive or negative) at the transition to/from unsteady flow is most easily observed in a control-space diagram. Other researchers, including Gavriely et al. (1989) and Patel (1993), have presented their results only in terms of pressure difference vs. flow-rate, rather than on two axes of pressure, so it cannot be ascertained whether they observed an equivalent divergent instability. Aside from this large unattainable zone, the control-space diagram shows trends in the

regions of oscillation modes. At the lower right hand corner (high  $p_u$  and low but positive  $\bar{p}_{e2}$ ), there exists a large region of LU-type oscillations; these are low-frequency oscillations that have proportionally a very brief collapse phase (illustrated in Fig. 1(b)). Moving radially outward from this LU-region the tube tends to collapse more times per cycle (LU→LU2→LU3, etc.), causing the tube to spend an increasing proportion of time in the collapsed state (LUn→LDn). As the number of collapses per cycle increases, their relative amplitude diminishes, until they are deemed too small to count. When the external pressure overwhelms the tube, the oscillations subside and the tube remains in a continuously collapsed state. In some instances, small noise-like fluctuations about the collapsed state were seen (nf), which corresponded to a standard deviation of the  $\bar{p}_2$  waveform greater than 0.5 kPa.<sup>3</sup> A small region of high-frequency oscillations (43–52 Hz) was observed at the high- $p_u$  end of the diagram, just prior to continuous collapse.

Such a large variety of distinct oscillation modes as that shown in Figs. 1 and 2 has its counterpart only in our previous observations on the thick-walled uniform tube (Bertram and Butcher, 1992a; Bertram and Castles, 1999). Greatly varied oscillations have not been reported by other groups. Gavriely et al. (1989), working with air-flows through thick-walled tubes (inside radius to wall-thickness ratios of 1.7 and 3, compared with 6 for the present thin-walled tube), observed only one type of oscillation which on grounds of associated theoretical work (Grotberg and Gavriely, 1989) was termed ‘flutter’. The oscillations were of very high frequency (260–750 Hz) relative to those observed here, and were accompanied by ‘loud honking sounds’. It was submitted that flutter may be the mechanism for the generation of respiratory wheezes. Patel (1993) recorded similar high-frequency flutter oscillations for air-flow (300–400 Hz). The frequency of oscillations in collapsible-tube flow is certainly related to the density of the transported fluid, both insofar as this affects the inertia of the downstream flow and, by setting whether the wall or the fluid is the predominant local inertia, dictating whether tube oscillation or tube-wall flutter is the governing mechanism (Pedley and Luo, 1998).

As an aside, ‘tube oscillation’ is here used in lieu of a better term. The theoretical literature accepts that the mechanism behind this type of oscillation is distinct from flutter. Grotberg (1994) defined the process as involving ‘relaxation oscillations of the choke point as it moves upstream, opens, and then reforms downstream’, and termed it milking after Bertram (1982). Oscillations in which the tube throat moves visibly along the tube during the cycle do indeed suggest this description. In addition to flutter, Patel observed an oscillation mode in which the tube throat (choke point) moved axially up and down the tube. Visible ‘milking’ was also recorded by Bertram and Chen (2000), who further classified these oscillations based on the number of tube throats. The original suggestion by Bertram (1982) was motivated by observing the oscillations of a uniform tube of red rubber. Milking was displayed particularly prominently in a tube consisting of bicycle-tyre inner tubing where the frequency of oscillation was slowed to extremely low values by unusually high inertia up- and downstream (Bertram, unpublished observations). Apart from Patel’s, all these observations concern aqueous flow. The only problem with adoption of the term to distinguish all collapsible-tube oscillations that are not flutter is that the throat does not always move sufficiently to be obvious. The mechanism in question is indeed thought to underlie all the observations of relatively thick-walled uniform silicone-rubber tubes by Bertram and colleagues over several years, but actual throat movement is all but imperceptible under some operating conditions. An approximate measurement of the extent at one operating point was made by Bertram et al. (1994); in this case it was some 3.5% of tube length, but often is very much less. Substantial throat movement was not visible in the present uniform-walled tube.

Returning to the current control-space diagrams (Fig. 2), as one travels up a  $p_u$  column, the frequency of the oscillations tends to increase within each region. Although Patel (1993) did not plot an equivalent diagram, he reported that when  $p_c$  was raised the frequency of oscillation increased within a certain mode. The control-space diagrams in refs. I and II are also in broad agreement with this trend. The clinical significance of this observation is that in a bronchioconstrictive event the patient may be monitored by measuring the wheeze frequency (Gavriely et al., 1989).

#### 4.2. Flow-rate limitation

The flow-limitation behaviour of the thin-walled tube bore qualitative resemblances to some aspects of that of each of the previously examined tubes. Flow-rate limitation was here mostly associated with large-amplitude self-excited oscillations for both increasing and decreasing external pressure, to a greater extent even than in the tapered-thickness tube (ref. II). In contrast, the uniform thick-walled tube largely eschewed periodic oscillation of substantial magnitude (ref. I), and the fairly thick-walled tube used by Gavriely et al. fluttered only along restricted segments of a few of their flow-rate limitation curves. This finding suggests that the likelihood that the tube will persist in a large-amplitude oscillatory state during flow-rate limitation increases with tube compliance.

<sup>3</sup>A threshold of 2 kPa was defined for nf in the thicker tubes of previous experiments—see Bertram and Butcher (1992a).

At the transition to and from flow-rate limitation, the magnitude of the change in flow-rate relative to the flow-limited flow-rates themselves, was large for increasing external pressure (flow-rate reduction), corresponding to behaviour in the thick-walled tube. For decreasing external pressure (leaving the flow-limited state), the increase in flow-rate at transition was small, the flow-rate having in most cases progressively increased already as the pressure drop came down. This behaviour corresponds qualitatively to that of the tapered-thickness tube, and represents a pronounced ‘negative effort dependence’ while flow-rate-limited, relative to the case for increasing external pressure. However, some degree of negative effort dependence was observed in all three tubes.

The behaviour during reduction of external pressure in the thin-walled tube (Fig. 3(b)) was complex, with apparently two broad possibilities available, depending on the value of upstream transmural pressure  $\bar{p}_{e1}$ : one, at the higher  $\bar{p}_{e1}$ -values (all the *negative* transmural pressures as usually defined—inside minus outside—but also at +2 kPa), corresponds to that seen when increasing external pressure in the thin tube and to that seen in the thick tube irrespective of direction of external pressure variation. The other, as just detailed, corresponds to that observed in the tapered-thickness tube; this behaviour, emphasizing negative effort dependence during flow-rate limitation instead of a major increase in flow-rate on leaving that state, occurred at negative  $\bar{p}_{e1}$  (positive transmural pressure at the upstream end of the tube) beyond –4 kPa. Behaviour thus switched over near  $\bar{p}_{e1} = 0$ . One would expect zero itself to have no significance for the tube; the important threshold would be that negative value of transmural pressure just sufficient to offset the tube’s own stiffness and bring it to the brink of collapse. That value would be approximately three times (Flaherty et al., 1972) the normalising pressure unit of 1.17 kPa (see Methods), i.e.  $\bar{p}_{1c} = -3.5$  kPa. It is unclear why behaviour should instead change at around  $\bar{p}_{1c} = +4$  kPa.

#### 4.3. Hysteresis

As in the thick-walled uniform tube which first forced us to separate results for increasing and decreasing external pressure, the thin-walled uniform tube here displayed strong hysteresis. The two contrasting behaviours discussed in the previous section, one of which occurred only when reducing external pressure, is perhaps the most striking example, and the one which is unique to the thin-walled tube. The other major manifestation parallels the thick-tube behaviour precisely: keeping to a suitably chosen single value of  $\bar{p}_{e1}$  throughout, the tube would resist collapse until a high flow-driving pressure was reached, then the curves of pressure drop vs. flow-rate would show a dramatic reduction in flow-rate as transition to flow-rate limitation occurred. Instead of reversing along this same path when external pressure was lowered, the tube would instead remain collapsed and flow-limited until much lower values of flow-driving head were reached. The prominence of hysteresis here is a consequence of the shape of the pressure–area relation for a uniform silicone-rubber collapsible tube (Bertram, 1987), which combines material hysteresis with almost infinite compliance between buckling and opposite-wall contact. A tapered-stiffness tube has a more progressive collapse (Fig. 1, ref. II), and consequently the effects of the undiminished material hysteresis are less dramatic. Similarly, the uniform tubes examined by Kekecioglu et al. (1981) and by Yamane and Orita (1994) retained finite stiffness between buckling and opposite-wall contact, and therefore were not subject to such dramatic hysteretic effects. However Yamane and Orita did report hysteresis at low flow-rates, and also that initial conditions affected the operating point at high flow-rates.

#### 4.4. Nonuniqueness

As in the tapered tube, clusters of points sharing the same pair of upstream transmural pressure and upstream head values were observed. Thus flow-limited flow-rate for a given pressure drop was again not uniquely determined by upstream transmural pressure. In each tube, it has been shown that the behaviour is a consequence of the nonmonotonic dependence of upstream transmural pressure on external pressure. In the thin tube, this was the case at all values of flow-driving pressure  $p_u$  beyond 13 kPa. In the tapered-thickness tube, it was so at all values where the relation was investigated. The relation was not investigated for the thick-walled tube of ref. I; it is an open question whether such a nonmonotonic dependence would be found, although we believe it would. This investigation identified a small extra facet of cluster behaviour compared to the tapered tube, as a result of a protocol which allowed the  $(p_e, \bar{p}_{e1})$ -relation results to be used to add points to the flow-rate limitation curves. What we term pre-transitions to flow-rate limitation were thereby identified as possible if sufficient departure from the nominal  $\bar{p}_{e1}$ -value was allowed *en route*.

Nevertheless, the extent of the variation in flow-rate between the points forming the nonuniqueness clusters, here as in the tapered-stiffness tube of ref. II, remains always small in comparison with that which was found in the tapered-stiffness tube with airflow by Patel. We speculate that change of oscillatory mode can produce much more dramatic variations in flow-limited flow-rate when flutter underlies the oscillation.

#### 4.5. Nondimensionalisation

It is generally accepted that an appropriate nondimensionalisation scheme for collapsible-tube flows is that based on the pressure unit  $P_k = E(h/R)^3/12(1 - \nu^2)$ , where  $E$  and  $\nu$  describe the material in simple isotropic infinitesimal-strain terms and the wall thickness  $h$  and radius  $R$  describe the tube. The expression is based on a description of the bending stiffness of the tube wall. A unit of speed is then found as  $\sqrt{P_k/\rho}$ ,  $\rho$  being the fluid density, and hence a unit of flow-rate. Tube wall thickness thus has a marked affect on the dimensionless values of both pressure and flow-rate. Comparing the thick-walled tube of ref. I with the thin-walled tube of the present experiments, the dimensionless range of  $p_u$ ,  $\bar{p}_{e2}$ ,  $\bar{p}_{12}$ , etc., occupied by a given experimental range of values for the thick tube is only some 16% of that occupied by the same experimental values for the thin tube. Similarly, the thick-tube experiments would have spanned only some 36% of the dimensionless range occupied by equivalent experimental values here. The experimental ranges were not the same; in deference to the greater fragility of the thin-walled tube, a maximum  $p_u$  of 100 kPa was used here, whereas up to 200 kPa was employed with the thick-walled tube. But in considering the differences in behaviour manifested by the two uniform tubes, it is appropriate to remember that the thin-walled tube experiments spanned some three times the dimensionless space in each linear direction on both the control-space diagrams of Figs. 2 and 4 and the pressure-drop/flow-rate diagrams of Fig. 3.

#### 5. Conclusions

Taking the outcomes together, it is established that a nonunique relation between upstream transmural pressure and flow-limited flow-rate at a given pressure drop is *not* a feature peculiar to tapered-stiffness tubes, as had previously appeared. Rather it now seems characteristic of more compliant tubes, and probably has not been observed in past investigations of uniform thin-walled tubes simply because of technique. Stiffness taper however mitigates against prominently hysteretic behaviour, which was seen (in differing manifestations) in both uniform tubes only. Self-excited oscillation accompanied flow-rate limitation in both the tapered and the thin-walled tube; this is in line with findings elsewhere for air-flow in tapered tubes. The finding in the thick-walled tube that oscillation does not always accompany flow-rate limitation likewise parallels a finding of others with air-flow. Prominent reductions in flow-rate when collapse and flow limitation occur have now been seen in our thick tube (both directions of external pressure variation), our thin tube (increasing external pressure only), and a tapered tube with air-flow elsewhere. However, instead increased degrees of negative effort dependence were seen in our tapered tube with aqueous flow and in our thin tube when external pressure was being decreased, at least at most positive upstream transmural pressures. A unifying principle has yet to be identified here.

Tubes of tapered stiffness thus seem less unique in most of their properties as a consequence of this investigation. This finding may disappoint those who believe that the behaviour of uniform tubes is dominated by the abrupt disappearance of compliance at the junction with the downstream pipe, and therefore unphysiological. Certainly, any horizontal uniform tube subjected to uniform external pressure has its throat, the site of most collapse and most vigorous oscillation, necessarily located as close to that discontinuity as tube wall bending allows. We have previously shown that abolition of this situation by compressing and collapsing only an intermediate segment of a longer flexible tube does not change the dynamics qualitatively or to a great extent (Bertram and Butcher, 1992b). The results of this latest investigation thus reinforce our previous belief that uniform tubes do indeed portray physiologically relevant behaviour, albeit in idealised circumstances where the dynamics that may be suppressed by various added complexities in vivo can be brought out. However, it must be allowed that the investigation of the tapered-stiffness tube in ref. II presented results mainly from the regime where the qualitatively unique feature of the tube that stiffens progressively in the streamwise direction, namely the mobile throat, no longer applied. In the regime where the throat was able to migrate away from the downstream end, four types of weak milking oscillations were identified, and these were accompanied by just-perceptible further minima of tube area upstream of the throat (see ref. II for details). Although careful observations were made of many operating points, and a control-space diagram of the regime was constructed, Bertram and Chen found it impossible to analyse the regime to the same level of detail as when the throat was again at the downstream end, because of the great variability of these very weak oscillations. Ohba et al. (1998) have also reported briefly on observations from a tapered-stiffness tube in this regime. Very careful experiments on a tapered-stiffness tube with aqueous flow were conducted also by Jaekle (1987), but his focus was entirely on the potential for smooth (nonshock-like) transitions from super- to subcritical flow. Consequently his lengthy and otherwise excellent report does not consider the questions raised here. There is clearly scope for further experimentation on tapered-stiffness tubes in the mobile-throat regime.

## Acknowledgements

NSJE was funded by an Australian Research Council grant-funded scholarship. The experiments were conducted using apparatus acquired through successive Australian Research Council grants to CDB.

## References

- Bertram, C.D., 1982. Two modes of instability in a thick-walled collapsible tube conveying a flow. *Journal of Biomechanics* 15, 223–224.
- Bertram, C.D., 1987. The effects of wall thickness, axial strain and end proximity on the pressure–area relation of collapsible tube. *Journal of Biomechanics* 20, 863–876.
- Bertram, C.D., 1995. The dynamics of collapsible tubes. In: Ellington, C.P., Pedley, T.J. (Eds.), *Biological Fluid Dynamics*. The Company of Biologists Limited, Cambridge, pp. 253–264.
- Bertram, C.D., Butcher, K.S.A., 1992a. A collapsible-tube oscillator is not readily enslaved to an external resonator. *Journal of Fluids and Structures* 6, 163–180.
- Bertram, C.D., Butcher, K.S.A., 1992b. Possible sources of discrepancy between sphygmomanometer cuff pressure and blood pressure quantified in a collapsible-tube analog. *ASME Journal of Biomechanical Engineering* 114, 68–77.
- Bertram, C.D., Castles, R.J., 1999. Flow limitation in uniform thick-walled collapsible tubes. *Journal of Fluids and Structures* 13, 399–418.
- Bertram, C.D., Chen, W., 2000. Aqueous flow limitation in a tapered-stiffness collapsible tube. *Journal of Fluids and Structures* 14, 1195–1214.
- Bertram, C.D., Raymond, C.J., Pedley, T.J., 1990. Mapping of instabilities for flow through collapsed tubes of differing length. *Journal of Fluids and Structures* 4, 125–153.
- Bertram, C.D., Raymond, C.J., Pedley, T.J., 1991. Application of dynamical system concepts to the analysis of self-excited oscillations of a collapsible tube conveying a flow. *Journal of Fluids and Structures* 5, 391–426.
- Bertram, C.D., Sheppard, M.D., Jensen, O.E., 1994. Prediction and measurement of the area–distance profile of collapsed tubes during self-excited oscillation. *Journal of Fluids and Structures* 8, 637–660.
- Bonis, M., Ribreau, C., 1978. Etude de quelques propriétés de l'écoulement dans une conduite collabable. *La Houille Blanche* 4, 165–173.
- Elliott, N.S.J., 2000. Aqueous flow-limitation in a uniform thin-walled collapsible tube. B.E. Thesis, University of New South Wales.
- Flaherty, J.E., Keller, J.B., Rubinow, S.I., 1972. Post buckling behavior of elastic tubes and rings with opposite sides in contact. *SIAM Journal of Applied Mathematics* 23, 446–455.
- Gavriely, N., Shee, T.R., Cugell, D.W., Grotberg, J.B., 1989. Flutter in flow-limited collapsible tubes: a mechanism for generation of wheezes. *Journal of Applied Physiology* 66 (6), 2251–2261.
- Grotberg, J.B., 1994. Pulmonary flow and transport phenomena. *Annual Review of Fluid Mechanics* 26, 529–571.
- Grotberg, J.B., Gavriely, N., 1989. Flutter in flow-limited collapsible tubes: a theoretical model of wheezes. *Journal of Applied Physiology* 66 (6), 2262–2273.
- Jaekle Jr., D.E., 1987. Critical transitions associated with steady flow in collapsible tubes with varying wall stiffness. S.M. Thesis, Massachusetts Institute of Technology.
- Kekecioglu, I., McClurken, M.E., Kamm, R.D., Shapiro, A.H., 1981. Steady, supercritical flow in collapsible tubes. Part 1. experimental observations. *Journal of Fluid Mechanics* 109, 367–389.
- Ohba, K., Sakurai, A., Maekawa, K., 1998. Characteristics of the flow in collapsible tube with continuously varying compliance along the tube axis—its application to extracorporeal circulation. In: Matsuzaki, Y., et al. (Eds.), *Abstracts of the Third World Congress of Biomechanics*, Sapporo, Japan, p. 38.
- Patel, N.R., 1993. A study of flow limitation and flow-induced oscillations during airflow through collapsible tubing. B.S. Thesis, Massachusetts Institute of Technology.
- Pedley, T.J., Luo, X.Y., 1998. Modelling flow and oscillations in collapsible tubes. *Theoretical and Computational Fluid Dynamics* 10, 277–294.
- Shapiro, A.H., 1977. Physiologic and medical aspects of flow in collapsible tubes. *Proceedings of the Sixth Canadian Congress of Applied Mechanics*, Vancouver, pp. 883–906.
- Yamane, T., Orita, T., 1994. Hysteresis and multiplicity of collapsible tube flow. *Transactions of the Japan Society of Mechanical Engineers* 60 (571), 807–812 (in Japanese).